

Hypoxia mediated regulation of mitochondrial transcription factors: Implications of hypertensive renal physiology

Bhargavi Natarajan¹, Vikas Arige¹, Abrar A. Khan¹, Santosh Reddy^{2,3}, Manoj K. Barthwal², and Nitish R Mahapatra^{1*}

1 - Department of Biotechnology, Bhupat and Jyoti Mehta School of Biosciences, Indian Institute of Technology Madras, Chennai 600036, India.

2 - Pharmacology Division, CSIR-Central Drug Research Institute, Lucknow 226031, India.

3 - Academy of Scientific and Innovative Research (AcSIR), New Delhi 110025, India.

*Correspondence to Dr. Nitish R. Mahapatra: Department of Biotechnology, Bhupat and Jyoti Mehta School of Biosciences, Indian Institute of Technology Madras, Chennai 600036, India. nmahapatra@iitm.ac.in; Tel. 91-44-2257-4128

Abbreviations

mtTFs, mitochondrial transcription factors; OXPHOS, oxidative phosphorylation; ATP, adenosine triphosphate; ETC, electron transport chain, TiH, tubulointerstitial hypoxia; PGC-1 α – peroxisome proliferator activated receptor gamma coactivator 1-alpha; SHR, spontaneously hypertensive rats; WKY, Wistar Kyoto rat; HIF-1 α , Hypoxia Inducible factor 1 α ; HREs, hypoxia response elements; mtDNA, mitochondrial DNA; ChIP, chromatin immunoprecipitation; bp, base pair.

Abstract

Introduction: Kidneys are organs with high resting metabolic rate and low tissue pO_2 due to enhanced mitochondrial oxygen consumption and ATP production for active solute transport. Such enhanced mitochondrial activity leads to progressive hypoxia from the renal cortex to medulla. Renal tubulointerstitial hypoxia (TiH) is severe in hypertensive rats due to increased sodium reabsorption within their nephrons. However, expression of mitochondrial transcription factors (mtTFs) (viz. Tfam, Tfb1m and Tfb2m) and mitochondrial biogenesis is not reported during hypoxic conditions.

Materials and Methods: Transcriptional regulation of Tfam, Tfb1m and Tfb2m under acute hypoxia was studied using promoter-driven luciferase assays, qPCR, western blotting and Chromatin Immunoprecipitation.

Results: The expression of HIF-1 α , PGC-1 α , Tfam, Tfb1m, Tfb2m and OXPHOS proteins were higher in hypertensive rats as compared to the normotensive ones. Additionally, studies on NRK52e cells show that acute hypoxia increases the expression of these genes. We also observed a positive correlation between HIF-1 α and mtTFs in human tissues. Furthermore, we report for the first time, that HIF-1 α binds to promoters of Tfam, Tfb1m and Tfb2m genes and augments their promoter activity.

Conclusion: Hypertensive rats, with increased TiH show enhanced expression of mitochondrial proteins. HIF-1 α directly binds to and increases promoter activity of mtTFs. Acute hypoxia induces the expression of mtTFs and probably promotes mitochondrial biogenesis in NRK52e cells.

Keywords: Tubulointerstitial Hypoxia, Tfam, Tfb1m, Tfb2m, acute hypoxia, transcriptional regulation,

INTRODUCTION

The role of kidneys in hypertension was first proposed by Guyton, who developed a model proving the influence of renal natriuresis and diuresis on blood pressure¹. Although this theory is now challenged by identification of several non-renal factors as proposed by the mosaic theory^{2, 3}, the indelible impact of kidneys on blood pressure regulation remains unchanged. Active solute transport by kidneys demands energy. This increases oxygen consumption and thereby causes hypoxic environment in the renal epithelial cells. Therefore, it has been proposed that kidneys function at the brink of anoxia^{4, 5}. Hypoxia triggers the reprogramming cellular activities to meet the energy requirement^{6, 7}. Moreover, increased activity of membrane transporters in kidneys of Spontaneously Hypertensive Rats (SHR) exacerbates tubulo-interstitial hypoxia (TiH) which is milder in the Wistar-Kyoto normotensive rats (WKY)⁸. Kidney transplantation studies provide evidence that genetic factors within the kidney might be responsible for the onset of hypertension in the spontaneously hypertensive rats (SHR) when compared to Wistar-Kyoto normotensive rats (WKY)⁹⁻¹². Despite receiving 20% of the cardiac output, the exorbitant metabolic requirement of the kidneys results in low oxygen tension within the nephrons^{13, 14}. Consistent with the heart, the resting metabolic rate of the kidneys is also high necessitating a high number of healthy mitochondria to meet the ATP demand for solute transport.

Multiple studies demonstrate renal mitochondrial dysfunction in hypertensive rodent models (viz. SHR and Dahl Salt Sensitive rats)¹⁵. Experiments performed with adult SHR and WKY rats reveal defective renal oxygenation and increased mitochondrial oxidative stress in SHR as compared to WKY^{16, 17}. Moreover, studies have reported previously that the oxygen consumption rate and ATP synthesis are higher in the proximal tubular cells of young SHR when compared with age-matched WKY^{14, 18, 19}. However, the renal expression profile of many mitochondrial genes that could explain the enhanced ATP production in young pre-

hypertensive SHR is largely elusive. It is well established that hypoxia and oxidative stress are primary renal abnormalities in SHR²⁰, and we speculate that these stresses might alter the expression of mitochondrial genes. Specifically, the expression of mitochondrial transcription factors under hypertensive and hypoxic conditions remains unexplored.

Mitochondrial transcription factors, viz. Tfam, Tfb1m and Tfb2m (mtTFs) are crucial players in mitogenesis as well as the expression of mitochondrial genome²¹. The mitochondrial genome of mammals is a ~16 kb circular genome coding for 37 genes (2 rRNA genes, 22 tRNA genes and 13 protein coding genes). Additionally, mitochondrial DNA (mtDNA) contains a ~1 kb control region harboring an origin of replication and three adjacent promoters enabling replication and transcription of the genome²². Tfam enables both replication and transcription of the mitochondrial genome by binding to the mitochondrial DNA and RNA polymerases, namely PolG and Polrmt respectively. Tfam has also been reported to cooperatively bind to the entire mitochondrial DNA in order to enable compaction, thereby protecting it from ROS-induced damage²³. Tfb2m binds to Polrmt and facilitates promoter recognition²⁴.²⁵. Tfb1m carries out the first step in mitochondrial ribosome biogenesis and therefore aids in mitochondrial protein translation.²⁶. Peroxisome-proliferator-activated-receptor- γ -co-activator-1 α (PGC1 α), the master regulator of mitochondrial biogenesis drives the transcription of mtTFs and other mitochondrial genes in association with Nuclear Respiratory Factors 1&2 (NRF1 and NRF2) and Sp1^{27, 28}.

In this study, we aim to study the expression of mitochondrial transcription factors and mitochondrial genes in the kidney of SHR and WKY. Furthermore, since kidneys are hypoxic organs requiring more energy, we study in detail, the influence of hypoxia on the expression of these genes using an in vitro cell culture model at the transcriptional and translational levels.

MATERIALS AND METHODS

Rat strains

In order to study the early changes in the hypertensive kidneys, the renal tissues from 4-6-week-old Spontaneously Hypertensive rats (SHR) and Wistar Kyoto normotensive rats (WKY) were dissected and stored in RNA-later solution to prevent RNA and protein degradation. For TEM analysis, the rats were perfused with 3% glutaraldehyde before dissection of the kidneys. The animal experiments were approved by the Institute Animal Ethics Committee at Indian Institute of Technology Madras.

Generation of rat Tfam, Tfb1m and Tfb2m promoter-luciferase reporter constructs

Promoter regions (~1.3 kb) of mitochondrial transcription factors were PCR-amplified using genomic DNA isolated from Wistar-Kyoto rats as template, primers specific to the promoters of Tfam, Tfb1m & Tfb2m (Table 1) and Phusion® High Fidelity DNA polymerase (Finnzymes, USA) at an annealing temperature of 62°C. DMSO at a concentration of 3% was added to the reaction mixture. The purified PCR products and the pGL3Basic vector (Promega, USA) with firefly luciferase reporter were double digested with KpnI and XhoI restriction enzymes (New England Biolabs, UK). Ensuing this, the vector was incubated with Calf Intestinal phosphatase (CIP) (New England Biolabs, UK) for 15 minutes at buffer conditions specified by the manufacturer in order to remove 3'-OH overhangs. After additional purification of the inserts and vector, they were ligated using T4 DNA Ligase (ThermoFisher, USA). The ligation reaction was set at 10°C in an insulated water bath for 12 hours so that the gradual increase in temperature during this time will let the ligase find an ambient condition to ligate the insert and vector. Ligation mixture was subsequently

transformed into DH5 α ultracompetent cells and the resulting colonies were screened to obtain the desired clones. Additionally, the clones were sequenced for confirmation.

In silico prediction of transcription factor binding sites in the mitochondrial transcription factors' promoters

This work aims to identify the hypoxia induced expression of mitochondrial transcription factors. Therefore, online transcription factor binding site prediction tools were used to specifically find binding sites for HIF1 α , known as Hypoxia Response Elements (HREs), in the promoters of Tfam, Tfb1m and Tfb2m. The promoter sequences obtained from UCSC genome browser were given input sequences and HIF1 α was specifically selected wherever possible. The scores predicted by the different tools for various HIF1 α binding sites are listed in Table 2. The conservation of HREs across various mammalian species was analyzed. In order to accomplish this, the sequence of the mitochondrial transcription factors' promoters from Human, Rat, Mouse, Chimp, Orangutan, Gorilla, Rhesus Monkey, Green Monkey, Gibbon, Macaque, Dog, Pig and Cow were obtained from UCSC genome browser or Ensembl. The GenBank/Ensembl accession IDs for these species are given in Table 3. These sequences were aligned using ClustalW and the alignment file was analyzed using the GeneDoc software.

Cell culture and transfection

Authenticated Normal Rat Kidney epithelial cells (NRK 52e) were obtained from the Indian national cell-line and hybridoma repository at the National Center for Cell Sciences, Pune, India. Dulbecco's modified Eagle's medium with high glucose and glutamine (HyClone, USA) supplemented with 10% fetal bovine serum, streptomycin (100 mg/mL) and penicillin G (100 U/ml) (Invitrogen, USA) was used for culturing cells in 25-cm² tissue culture flasks,

60 mm or 100 mm dishes as described previously²⁹. The cells were periodically tested for mycoplasma contamination through a PCR-based method. If contaminated, the cells were treated for three weeks with BM cyclins (Roche, USA) to get rid of contamination prior to performing our in vitro experiments. Transfections were done transiently in a 24-well plate using a peptide-based transfection reagent, Targefect F2 (Targeting Systems, USA), at a ratio of 1:1 wt/vol (DNA: Targefect F2). In each experiment, at ~70-80% confluency, 500 ng/well of Tfam-pro, Tfb1m-pro or Tfb2m-pro promoter-reporter construct was co-transfected with 250 ng/well of β -galactosidase expression plasmid serving as an internal control for transfection efficiency. Subsequently, the cells were subjected to acute hypoxia for two hours and lysed.

Acute hypoxic exposure and luciferase assay

12 h after transfection, cells were subjected to two hours of acute hypoxia. This was done by first placing the cells in a hypoxia chamber (BelArt, USA). Argon gas with 99% purity was infused for three mins to replace the existing oxygen to Argon. After this, the cabinet was sealed tightly and placed inside an incubator set to 37°C. Parallely, the cells to be kept under normoxic conditions were placed in the regular CO₂ incubator. The incubation under hypoxia was for two hours, ensuing which they were lysed for downstream assays. Luciferase assays were carried out using a luciferase assay buffer (100 mM Tris-acetate, pH 7.8, 10 mM magnesium acetate, 1 mM EDTA, pH 8.0, 3 mM ATP and 100 μ M beetle luciferin potassium salt) as described previously²⁹. The values obtained as relative luciferase units per second (RLU/s) were normalized with β -galactosidase activity and total protein estimated by Bradford assay. Such experiments were repeated thrice, and the data are expressed as percentage over control of a representative experiment.

RNA isolation and quantitative real-time PCR in NRK52e cells and rat model of essential hypertension

In order to determine the expression profile of mitochondrial genes in our animal model, kidney tissues from SHR and WKY were isolated from young animals aged 4-6 weeks and stored in RNA later. Either these tissues or NRK52e cells (cultured under normoxic or hypoxic conditions) were washed with 1X PBS and homogenized using TRIzol reagent (Takara, USA). RNA was isolated using NucleoSpin RNA isolation kit (Takara, USA). The total RNA thus obtained was subjected to DNase treatment to remove any remnant DNA. Subsequently, cDNA was synthesised using cDNA synthesis kit (Takara, USA) according to manufacturer's instructions. 20-40 ng of cDNA was used in each qPCR reaction and the fold change of expression with respect to the control (WKY normotensive rats or cells grown under normoxic condition) was calculated using the $\Delta\Delta C_t$ method as described previously²⁹. Primers specific for β -Actin was used as a house keeping control. The primers used for the mitochondrial genes profiled in this study are listed in Table 4.

DNA isolation and estimation of mitochondrial DNA content

In order to estimate mitochondrial DNA levels, the samples homogenised with Trizol for RNA isolation were used. After aspirating the aqueous phase containing RNA, 100% ethanol was added to the interphase and phenol-chloroform layer to precipitate DNA. Ensuing this, the samples were centrifuged at 200 rpm for 5 minutes at 4°C. The supernatant was discarded, and the pellet was washed twice with 0.1 M sodium citrate. The pellet obtained was then solubilised in DNase- and RNase- free water. Total DNA was then subjected to RNase treatment to remove traces of RNA contamination. Total DNA containing both nuclear and mitochondrial DNA and was used in qPCR reactions to quantify amount of mtDNA as done previously³⁰. The difference in the expression between SHR and WKY or

normoxic vs hypoxic condition was calculated using $\Delta\Delta C_t$ method using 18S rRNA as control.

Western blotting for various proteins in NRK52e cells and rat model of essential hypertension

Kidney tissues from SHR and WKY were isolated and washed with 1X PBS. The tissues were minced with RIPA buffer using a homogenizer. Sonication was performed at an amplitude of 30/s for 5 min in ice so as to breakdown the nucleic acids that might interfere with SDS-page and Western blotting. NRK52e cells were seeded in six well plate and exposed to hypoxia or normoxia for two hours. Supernatant was discarded and the cells were washed with 1X PBS prior to lysis using RIPA buffer. Lysates were subjected to gentle sonication at 30/s amplitude for 30 seconds. The proteins were then estimated using Bradford reagent (Bio-Rad, USA). 50 μ g of protein was separated in a 10% SDS-polyacrylamide gel by electrophoresis. The separated proteins were transferred on to a PVDF membrane (Pall Life sciences, Mexico). Pre-stained protein ladder of wide range (Abcam, USA) was used as a molecular weight marker. The membranes were then blocked and probed with different concentrations of primary antibody: Tfam (CAT#sc28200; Santa Cruz Biotechnology, USA), Tfb1m (CAT#ARP34544_T100; Aviva, USA), Tfb2m (CAT#ab13676; Abcam, USA), OXPHOS cocktail (CAT#ab110413; Abcam, USA), HIF1 α (CAT#ab463; Abcam, USA), PGC1 α (CAT#ab54481; Abcam, USA) and Vinculin (CAT#V9131; Sigma-Aldrich, St. Louis, USA). After washing 3 times with 0.05% 1X TBST for 10 min, incubation was done with HRP conjugated secondary antibody raised against goat (ab6741; Abcam, USA), mouse (CAT#115-035-003; Jackson ImmunoResearch, USA) or rabbit (CAT#111-035-003; Jackson ImmunoResearch, USA). Washing steps were performed again 3 times with 0.05% 1X TBST for 5 min. The blocking agent, primary and secondary

antibody dilutions and duration of incubation in each case is detailed in Table 5. The resulting chemiluminescence was detected using ECL substrate kit (Bio-Rad, USA). The band intensities were then quantified using ImageJ software.

Chromatin immunoprecipitation

ChIP assay was carried out as detailed earlier. Briefly, NRK52e cells were cultured in a 100 mm dish upto 90% confluency after which they were subjected to either hypoxia for two hours or not. Cells under both hypoxic and normoxic conditions were quickly washed with 1X PBS and crosslinked with 1% formaldehyde. Fixation was stopped using 0.125M glycine after which the cells were scraped and centrifuged at 3000 rpm for 7 min at 4°C to pellet the nuclei. Nuclear pellet was then lysed with nuclei lysis buffer. Sonication was carried out at an amplitude of 35/s for 30 min in order to shear the chromatin. Sheared chromatin was precleared using beads that were blocked with BSA and E. coli genomic DNA. The precleared chromatin was incubated with 5 µg of HIF1α (CAT#ab463; Abcam, USA) or Tfam (CAT#sc28200; Santa Cruz Biotechnology, USA) antibody (in 1X ChIP buffer supplemented with protease inhibitors) overnight at 4°C for immunoprecipitation. Parallely, the chromatin was also incubated with mouse IgG (CAT# I5831; Sigma-Aldrich, St. Louis, USA) and rabbit IgG (CAT# I5006; Sigma-Aldrich, St. Louis, USA) antibody as a negative control to account for non-specific interactions during immunoprecipitation. Pull down of antibody bound DNA-protein complexes was done using ChIP grade G-sepharose beads (Invitrogen, USA). After stringent washing steps using low salt buffer, high salt buffer, lithium chloride and TE buffer as described previously, DNA was eluted and reverse crosslinked using 5M NaCl. Subsequently purified DNA was used for PCR amplification using primers that flank potential binding sites for HIF1α and Tfam. The list of primer sequences is given in Table 6.

RESULTS

Expression of mitochondrial transcription factors is higher in the kidney cortex of SHR when compared to WKY

Since mitochondrial transcription factors are inevitable for proper mitochondrial function, the mRNA and protein expression of these genes, viz. Tfam, Tfb1m and Tfb2m were estimated in young SHR and WKY kidney tissues. Consistent with our initial hypothesis, real-time qPCR analysis revealed that in SHR, expression of mitochondrial transcription factors' mRNA levels are higher relative to WKY: Tfam (~3.2 fold; $p < 0.001$), Tfb1m (~2.1 fold; $p < 0.01$) and Tfb2m (~2.4 fold; $p < 0.01$) as shown in Figure 1A, 1B, 1C. In accordance with the mRNA expression profile, Western blotting indicated that the protein levels of mtTFs were also significantly elevated in SHR kidney as compared with WKY. Additionally, protein levels of subunits of the respiratory chain were also enhanced in SHR kidney, as evident from Figure 1D, 1E. These results indicate an increase in the expression of renal mitochondrial proteins in young pre-hypertensive SHR as compared to age matched WKY.

Increased expression of PGC-1 α and HIF-1 α in SHR kidneys

Kidney transplantation studies have made it clear that the kidneys of SHR are one of the main contributors of hypertension in the spontaneously hypertensive rats (SHR)¹². The SHR kidneys exhibit heightened sodium and water reabsorption relative to normotensive WKY counterparts^{31, 32}. These data suggest that, when compared with WKY, the SHR renal tubular cells require more energy for their function. Conceivably, these cells show augmented mitochondrial activity¹⁸. We hypothesized that higher mitochondrial activity in SHR might be accompanied by corresponding increases in several mitochondrial genes. To test this notion,

we estimated the mRNA and protein expression of the peroxisome-proliferator-activated-receptor-gamma-coactivator-1-alpha (PGC-1 α) which is the master regulator of mitochondrial biogenesis. In accordance to our hypothesis, we observed that PGC-1 α mRNA expression was ~4-fold ($p < 0.0001$) higher in SHR kidneys compared to WKY. Western blotting revealed correspondingly higher protein levels of PGC-1 α in SHR as compared to WKY (Figure 2A, 2B).

Previously, multiple studies have reported that increased mitochondrial activity increases oxygen consumption and causes intracellular hypoxia^{5, 33}. Additionally, kidneys are oxygen deficient organs since active solute transport increases their requirement of ATP⁵. To understand whether this phenomenon occurs in the kidneys of SHR and WKY, we estimated the expression of Hypoxia-Inducible-Factor-1-alpha (HIF-1 α) which is an indicator of cellular oxygen deficiency. Interestingly, both the mRNA and protein expression of HIF-1 α was higher in the SHR kidney by ~2-fold ($p < 0.0002$) and ~1.4-fold ($p = 0.16$) respectively as compared to WKY (Figure 2A, 2B). Our results support previous observations that SHR kidneys have high ATP demand and are deprived of oxygen.

Positive correlation between HIF-1 α , and mtTFs expression in rodent model of hypertension and human tissues

So far, we have seen that in comparison to WKY, SHR express higher amounts of PGC-1 α , mtTFs and HIF-1 α suggesting increased severity of renal tubulointerstitial hypoxia and ATP demand in these rats. We postulated that there might be a correlation between these expression patterns. To assess this, we utilized RNA-seq data of various human tissues obtained from the open-source GTex portal. Our correlation study revealed significant positive correlation between Tfam and HIF-1 α (Pearson's $r = 0.7088$; $p < 0.0001$), Tfb1m

and HIF-1 α (Pearson's $r = 0.7063$; $p < 0.0001$) and Tfb2m and HIF-1 α (Pearson's $r = 0.3962$; $p = 0.0048$). (Figure 2C, 2D, 2E).

Effect of acute hypoxia on the promoter activity, mRNA and protein levels of mtTFs

So far, we have observed in the rat model of hypertension that major mitochondrial proteins (viz. Tfam, Tfb1m, Tfb2m, PGC-1 α and OXPHOS subunits) are substantially higher in SHR as compared to WKY. Besides a significantly increased mRNA and protein expression of HIF-1 α in SHR in comparison to WKY, data from human tissues revealed a positive correlation between HIF-1 α , PGC-1 α and mtTFs. These data prompted us to carry out experiments to elucidate hypoxia mediated expression of mtTFs in an in vitro cell culture model. To this end, we transfected NRK52e rat kidney epithelial cells with mtTFs' promoter-luciferase reporter constructs for 12 hours following which they were exposed to acute hypoxia for two hours. Subsequently, cells were lysed and assayed for luciferase activity. We found that the mtTFs' promoter activity increases by several fold (Tfam: ~12fold; $p < 0.01$; Tfb1m: ~3.6 fold; $p < 0.001$; Tfb2m: 1.7fold; $p < 0.05$) ensuing acute hypoxia (Figure 3A, 3B, 3C).

Next, we wanted to know if the increase observed at the promoter level is sustained at the mRNA and protein levels. RNA and protein were isolated from NRK52e cells exposed to acute hypoxia. qPCR analysis showed heightened transcript levels of Tfam (1.4-fold; $p < 0.05$), Tfb1m (1.5-fold; $p < 0.05$) and Tfb2m (2.8-fold; $p < 0.05$) after exposure to acute hypoxia (Figure 3D, 3E, 3F). Similarly, acute hypoxia elevated the protein levels of mtTFs as revealed by immunoblotting. Successful induction of hypoxia was confirmed by Western blotting with antibody against HIF-1 α which increased upon inducing hypoxia. Interestingly, the expression of OXPHOS subunits as well as PGC-1 α were also higher during hypoxic conditions (Figure 3G).

Identification of multiple HIF-1 α binding sites in the promoter region of mtTFs and their conservation across mammals

Due to the strong positive correlation between HIF-1 α and mtTFs in human tissues as well as the rodent genetic model of hypertension used in our study, we speculated that HIF-1 α binding sites might be present and functional in the promoter region of mtTFs. We used extensive online tools for in silico prediction of HIF-1 α binding sites in the promoters of mtTFs. Multiple such tools predicted binding sites for HIF-1 α in many positions within the proximal promoter of mtTFs with good scores (Table 2). Figure 4A shows the consensus matrix of HIF-1 α . Interestingly, one HRE from each promoter was conserved across mammals suggesting a probable evolutionary importance (Figure 4B, 4C, 4D). The predicted scores and sequence of these conserved HREs are indicated below the consensus matrix in Figure 4A.

In vivo interaction of HIF-1 α with promoters of Tfam, Tfb1m and Tfb2m

In silico predictions have revealed four Hypoxia Response Elements (HREs) in Tfam, two each in Tfb1m and Tfb2m. Their positions are shown schematically in Figure 5A. It is possible that one or more of these sites are functional. In order to find out which of the predicted HIF-1 α binding sites are functional in vivo, we carried out chromatin immunoprecipitation assays in NRK52e cells after exposing them to two hours of acute hypoxia. Immunoprecipitation of crosslinked and sheared chromatin from normoxic and hypoxic cells was done using HIF-1 α and IgG antibodies. Immunoprecipitated DNA was extracted and used to perform qPCR reactions. Primers were synthesized to span one or more of these HREs in the promoter regions as shown in Figure 5A. These primers are listed in Table 6. qPCR revealed enhanced binding of HIF-1 α to HRE1/2 of Tfam promoter during acute hypoxia (~1.3-fold; $p < 0.005$). However, there was no significant difference in HIF-1 α

binding to HRE3 and HRE4 of Tfam. Similarly, acute hypoxic condition increased HIF-1 α binding to the HRE1 of Tfb1m promoter (~1.2 fold; $p<0.05$) and HRE2 of Tfb2m promoter (~2-fold; $p<0.05$). Of note, HRE2 of Tfam, HRE1 of Tfb1m and HRE2 of Tfb2m are conserved across all mammals (Figure 3B, 3C, 3D)

In vivo interaction of Tfam with mtDNA

Tfam is known to take part in replication and transcription of the mitochondrial genome. Additionally, it also serves to coat the entire mtDNA in a histone-like manner so as to protect it from ROS-induced damage³⁴. In order to investigate the functional significance of enhanced expression of Tfam after hypoxia, we carried out ChIP assay after acute hypoxic stress. NRK52e cells were cultured at normoxia or exposed to hypoxia for two hours. Chromatin was immunoprecipitated using Tfam and IgG antibodies. The immunoprecipitated DNA was used in qPCR reactions in order to observe differential binding of Tfam to various regions of mtDNA. Two regions with 16S rRNA and ND5 genes of the mitochondrial DNA was chosen to test for Tfam binding. Primers were designed flanking these regions in order to test for Tfam binding (Table 6). We observe that Tfam binding to these regions of 16S rRNA and ND5 regions of mtDNA is significantly enhanced (~3-fold and 5-fold, respectively; $p<0.001$) upon exposure to acute hypoxia.

Functional consequence of increased expression of mitochondrial transcription factors

Till now, we have established that HIF-1 α directly binds to sites on the promoters of mitochondrial transcription factor and enhances gene expression during times of acute hypoxia. Additionally, we have also shown that binding of Tfam to mtDNA is enhanced during hypoxia. As stated earlier, enhanced Tfam binding to mtDNA could be for preventing ROS-induced damage. However, it is also possible that Tfam functions to enhance rates of

replication and transcription within the organelle. In this direction, mtDNA and mtRNA were quantified in NRK52e cells that were subjected to acute hypoxia. This was accomplished by qPCR analysis of three mitochondrial genes viz. 16S rRNA, ND5 and ND6. These genes were chosen since the transcription of each of these is from three of the adjacent promoters located within the D-loop (non-coding regulatory region) of mtDNA²². q-PCR analysis revealed augmented mtDNA copies as evident from fold expression of 16S rRNA (~2.2 fold; $p < 0.05$; Figure 6A), ND5 (~4-fold; $p < 0.001$; Figure 6B) and ND6 (~4-fold; $p < 0.0001$; Figure 6C) after acute oxygen deprivation. Correspondingly, we observed significantly enhanced expression of mtRNA apparent from the expression of 16S rRNA (~1.7-fold; $p < 0.01$; Figure 6D), ND5 (~3.3-fold; $p < 0.001$; Figure 6E) and ND6 (~3-fold; $p = 0.08$; Figure 6F). The primers used to analyze these genes are listed in Table 4. From these results, we propose that acute hypoxia possibly leads to augmented rates of replication and transcription of the mitochondrial genome. Moreover, this is followed by enhanced protein translation within the mitochondria as shown in Figure 4G.

Hypertensive rats exhibit increased mitochondrial gene expression

As stated earlier, SHR kidneys tend to be more hypoxic due to increase in ATP demand and oxygen consumption when compared to WKY. Additionally, our in vitro experiments suggest that short-term oxygen deprivation increases replication and transcription of mitochondrial genome. To find out if this holds true in our animal model of genetic hypertension whose kidneys are more hypoxic, we isolated total DNA and total RNA from the kidney tissues of SHR and WKY for expression analysis by qPCR. As shown in Figure 7A, 7B, 7C, mtDNA levels estimated using primers for 16S rRNA, ND5 and ND6 are elevated by ~3-fold in SHR ($p < 0.01$, $p = 0.05$ and $p < 0.05$ respectively). Furthermore, by performing qPCR analysis using total RNA, we demonstrate that the 16S rRNA (~1.8-fold; $p < 0.01$), ND5 (~3.8-fold; $p < 0.05$)

and ND6 (~3.6-fold; not significant) are more abundant in the hypertensive rat kidney in contrast to the normotensive rat kidneys as seen from Figure 7D, 7E, 7F. Therefore, the differences in the extent of hypoxia reported between SHR and WKY kidneys influence the expression of their mitochondrial genome and mitogenesis in these tissues.

DISCUSSION

Overview

Tubulo-interstitial Hypoxia (TiH) is a major instigator of renal malfunction and a contributing factor for many kidney diseases such as Chronic Kidney Disease (CKD), Acute Kidney Injury (AKI), End Stage Renal Disease (ESRD), etc. Interestingly, TiH has been implicated in hypertension induced renal malfunction and other types of nephropathy⁵. Of note, TiH is often accompanied by mitochondrial dysfunction^{35, 36}. Particularly, TiH is anteceded by oxygen deficiency resulting from increased oxygen consumption by mitochondria in renal tubular epithelial cells⁵. However, the effect of renal TiH on mitochondrial biogenesis is partially understood. In this study, we use a cell culture model of acute hypoxia and a rodent model of hypertension (SHR and WKY) to gain insights about mitogenesis during TiH. Our results indicate that the expression of crucial mitochondrial proteins encoded by the nuclear and mitochondrial genome is higher in the hypoxic kidney of SHR in contrast to WKY and also under acute hypoxia *in vitro* as compared to normoxic conditions.

Kidneys of young, pre-hypertensive SHRs exhibit augmented mitochondrial proteins

Kidneys are one among the organs that exhibit a high resting metabolic rate, thereby requiring excessive energy for efficient functioning^{37, 38}. Moreover, renal tubular epithelial cells have low glycolytic capacity and rely majorly on fatty acid oxidation (FAO) as source

of energy³⁹. Thus, proper mitochondrial function is essential in order to maintain adequacy of salt-water reabsorption. TiH has been observed in the hypertensive rodents (SHR) as opposed to the normotensive ones (WKY). As stated earlier, Increased TiH has been proposed to arise from decreased oxygen utilization efficiency in SHR. Additionally, SHR kidneys have been shown to carry out increased sodium reabsorption. In this study, we initially focused on mitochondrial biogenesis in SHR and WKY since mitochondrial health is imperative for active solute transport within the nephrons. To this end, we analyzed the expression of genes indicative of mitochondrial activity and abundance, viz. PGC-1 α , Tfam, Tfb1m and Tfb2m (mtTFs) in the kidneys of SHR and WKY. We observed that the renal abundance of PGC-1 α and mtTFs was significantly higher in SHR as compared to WKY. Correspondingly, the expression of mtDNA, mtRNA and ETC subunits were also elevated in the SHR kidneys in comparison to WKY. Furthermore, we observed that the expression of OXPHOS proteins (using a cocktail antibody) was augmented in SHR relative to WKY. These observations are in line with studies by Lee et al¹⁸ who have demonstrated increased mitochondrial activity in young SHR compared to WKY. These authors postulate that there is enhanced flux of acetylCoA into mitochondria of SHR kidney epithelial cells due to augmented expression and activity of pyruvate dehydrogenase. AcetylCoA, a precursor of tricarboxylic acid cycle (TCA cycle), promotes mitochondrial function in SHR¹⁸. Taken together, these results suggest that renal epithelial cells from young SHR exhibit enhanced mitochondrial function as compared to the normotensive WKY rats. Lee et al¹⁸ provide evidence that this is due to increased glycolysis and increased flux of pyruvate and acetyl-CoA. However, considering that renal cortical cells meet majority of their energy by FAO⁴⁰, it is possible that FAO is increased in SHR renal cortical cells, which would also increase the flux of acetyl-CoA into mitochondria. Increase in the mitochondrial proteins could thus be purported to aid in increased FAO and ATP synthesis. Several studies provide physiological evidence of increased ATP demand in

SHR kidneys. For example, it has been reported that the activity of Na^+/K^+ -ATPase pumps in renal cells of pre-hypertensive rats is higher than the normotensive rats⁴¹. Moreover, perfusion of isolated kidneys from 3-month SHR and WKY revealed higher sodium reabsorption in SHR kidney³¹. Multiple studies report pathological increases in salt and water reabsorption by SHR kidneys⁴²⁻⁴⁵. In addition, efficiency of sodium transport (total sodium transported per molecule of oxygen consumption) is compromised in SHR, leading to further increase in ATP demand¹⁴. Indeed, treatment with furosemide to reduce salt reabsorption, increases the cortical and medullary oxygenation in rats⁴⁶.

HIF-1 α expression is higher in SHR and positively correlates with the expression of mtTFs

In order to understand whether TiH is prevalent in renal cells of SHR and WKY, we measured the expression of HIF-1 α . Conceivably, HIF-1 α levels in the renal tissues was higher in SHR as compared to WKY. This is indicative of local oxygen deprivation, probably arising from increased oxygen consumption in the tissues of SHR. This is consistent with another study in which it observed that HIF-1 α ⁴⁷ is higher in the renal medulla where the tubular cells have to work against a greater concentration gradient in order to transport sodium. The increased oxygen consumption in SHR kidneys has also been attributed to inefficiency in oxygen utilization and NO bioavailability⁴⁸. Multiple research groups have observed decreased pO_2 in the kidneys in both normal and hypertensive cases. Therefore, our observation that HIF-1 α expression is more in SHR as compared to WKY, suggested enhanced oxygen deficiency in SHR. Thomas et al demonstrated that HIF-1 α ameliorates kidney oxygenation and improves mitochondrial function in mice model of subtotal nephrectomy³⁵. It is therefore possible that elevated expression of HIF-1 α in SHR as compared to WKY might serve to compensate for oxygen utilization inefficiency in these

rats. Furthermore, studies on rats that underwent subtotal nephrectomy, show that HIF-1 α improves renal oxygenation and promotes mitochondrial function³⁵. HIF-1 α has also been reported to be involved in the production of erythropoietin to stimulate production of RBCs⁴⁹. Indeed, the number of RBCs and hemoglobin in SHR and subjects with essential hypertension are observed to be higher than the corresponding normotensive counterparts^{14, 50}. Physiologically, such changes in SHR serve to increase renal oxygenation without increase in renal blood flow so has to avoid the concomitant increase in sodium load for reabsorption.

RNA-seq data retrieved from GTex portal for various human tissues reveals positive correlation between HIF-1 α and mtTFs across various human tissues. This data were obtained from healthy individuals. This suggests that HIF-1 α might regulate the expression of mtTFs under normal physiological conditions. Although this is not indicative of the protein levels of HIF-1 α , we speculate that transcription of HIF-1 α might be regulated by the amount of oxygen consumed, rather than a hypoxic condition. It is well established that high levels of AMP/ATP activate AMPK which in turn triggers HIF-1 α transcription⁵¹. Notably, AMPK activation is also indicative of energy demand of the cells. Therefore, it is possible that HIF-1 α transcription is regulated based amount of oxygen consumed and that its protein expression is stabilized under oxygen-deficient conditions. A positive correlation is thus understandable since mitochondrial transcription factors are directly related to ATP production and oxygen consumption. It has also been observed under physiologically normal oxygen concentrations PGC-1 α overexpression leads to intracellular oxygen deficiency and stabilizes HIF-1 α in skeletal muscles. HIF-1 α further activates its downstream targets and prepares the cells for oxygen deficiency arising from enhanced oxygen consumption⁷.

Acute hypoxia enhances the expression of mitochondrial transcription factors via HIF-1 α .

Data from rodent models of hypertension indicated a hypoxic environment in the SHR kidney. We also observed a strong positive correlation between HIF-1 α and mtTFs. Next, we asked whether there might be a functional link between them. Does hypoxia and thereby HIF-1 α influence the expression of mtTFs? In this direction, we sought to study the transcriptional regulation of mtTFs under conditions of acute hypoxia. Indeed, NRK52e exposed to acute hypoxia for two hours demonstrated augmented mtTFs' promoter activities. A concomitant increase in the mRNA and protein expression of these genes was also observed. Upon further analysis, we observed elevated expression of mitochondrial DNA, RNA and OXPHOS proteins after acute hypoxia. These results indicate increased mitochondrial replication, transcription and translation during acute hypoxia. Additionally, we found enhanced expression of PGC-1 α upon acute hypoxic stress.

HIF-1 α interacts with promoters of mtTFs to enhance their gene expression

In line with our in-silico predictions, ChIP analysis showed that HIF-1 α directly binds to the promoters of mtTFs on at least one of the predicted sites during hypoxia. Furthermore, these binding sites are conserved across mammals (viz. rat, mouse, human, pig, dog, cow, orangutan, chimpanzee, green monkey and rhesus monkey). Hence, it is possible that direct induction of mtTFs expression by HIF-1 α might occur in other mammals, suggesting that it is an evolutionarily crucial regulatory phenomenon. Therefore, our results enable us to allude that HIF-1 α -mediated enhanced expression of mtTFs during acute hypoxia might promote expression of mitochondrial genome in order to increase energy production.

Tfam binds to mtDNA during acute hypoxia

Mitochondria are major sites of ROS production and it is well established that hypoxic stress increases ROS levels within these organelles. ROS are known to cause DNA damage of various types. Although initially mtDNA were thought to be naked DNA susceptible to ROS-induced damage, subsequent studies have established that mtDNA is found in the form of nucleoids. Tfam is a major constituent of these nucleoids and is said to protect mtDNA from ROS induced damage apart from regulating the replication and transcription rates. Our ChIP assays reveal that hypoxia enhances the binding of Tfam to multiple sites on mtDNA. A highly plausible reason for this could be that Tfam coats mtDNA so as to prevent ROS-induced damage to the DNA. Such observations have been made before⁵². However, if the DNA is compacted, how would replication and transcription happen? A single mitochondrion is known to contain many copies of its genome. Tfam binding to mtDNA is cooperative in nature i.e. Tfam binds with greater affinity to DNA that already is bound to other molecules of Tfam⁵³. We speculate that out of multiple copies of the genome, most of it might be compacted while some still serve to enable gene expression. This kind of regulation is advantageous since if uncompact mtDNA is damaged, there are still many more to take its place enabling the cells to postpone the event of complete mitochondrial dysfunction. A similar observation has been made by Pastukh et al, where they show that oxidative modifications to mtDNA promotes Tfam binding to mtDNA under hypoxic conditions in pulmonary arterial endothelial cells. The time and severity of hypoxia in their experiments are similar to the time point that we chose. The authors show that such enhanced Tfam binding increases the mtDNA copy number since Tfam facilitates replication of mtDNA⁵⁴. This is in line with our observation of increased mtDNA copies after acute hypoxia. We also observe concomitant increases in mitochondria-encoded RNA. However, when the rate of transcription is calculated i.e. mtRNA/mtDNA, there seems to be a decrease

in the rate of transcription. These data corroborate with the study by Agaronyan et al, who report that mitochondrial replication and transcription are mutually exclusive in nature⁵⁵. Nevertheless, an overall increase in mitochondrial genome expression is observed.

CONCLUSIONS AND PERSPECTIVES

In this study, we have shown for the first time that acute hypoxia enhances the transcription of mitochondrial transcription factors by direct interaction of HIF-1 α with the promoters of these genes. The increase in HIF-1 α levels after acute hypoxia is accompanied by increase in PGC-1 α levels implicating that under our experimental conditions, mitochondrial biogenesis might be enhanced. Interestingly, Tfam binding to mtDNA is enhanced upon hypoxic stress. Additionally, our data indicates that short-term hypoxia increases the mitochondrial genome expression. These data are summarized in Figure 8.

In line with these in vitro data, the hypoxic SHR kidney, as revealed by enhanced expression of HIF-1 α exhibits greater expression of mtTFs than WKY. Furthermore, PGC-1 α is also expressed in higher amounts in SHR relative to WKY. Concomitant increases in mtDNA and mtRNA are also observed. This indicates heightened ATP requirements and increased oxygen consumption in SHR as compared to WKY. It should be noted that the animals that we used in our study are young, aged 4-6weeks when SHR's are still pre-hypertensive. We propose that in the early stages of hypertension progression, the organism's physiology still functions to meet the increased energy demand and tries to keep the kidneys keep functioning up to the best possible levels. Nevertheless, at a later age, ROS accumulation promotes inflammatory conditions might be responsible for reduction in mitochondrial proteins in renal tissue of SHR as compared to WKY^{20, 56}.

ACKNOWLEDGEMENTS

This work was supported by a grant from the Science and Engineering Research Board, Department of Science and Technology, Government of India to NRM (project number EMR/2017/004250). Research fellowships were received from Council of Scientific and Industrial Research (to BN), Department of Science and Technology (to VA), Ministry of Human Resource Development (to AAK), Indian Council of Medical Research (to SSR), Government of India.

REFERENCES

1. Guyton AC. The surprising kidney-fluid mechanism for pressure control--its infinite gain! *Hypertension* 1990; **16**: 725-730.
2. Page IH. The mosaic theory of arterial hypertension--its interpretation. *Perspect Biol Med* 1967; **10**: 325-333.
3. Evans RG, Bie P. Role of the kidney in the pathogenesis of hypertension: time for a neo-Guytonian paradigm or a paradigm shift? *Am J Physiol Regul Integr Comp Physiol* 2016; **310**: R217-229.
4. Heyman SN, Khamaisi M, Rosen S, *et al.* Renal parenchymal hypoxia, hypoxia response and the progression of chronic kidney disease. *Am J Nephrol* 2008; **28**: 998-1006.
5. Friederich-Persson M, Thorn E, Hansell P, *et al.* Kidney hypoxia, attributable to increased oxygen consumption, induces nephropathy independently of hyperglycemia and oxidative stress. *Hypertension* 2013; **62**: 914-919.
6. Debevec T, Millet GP, Pialoux V. Hypoxia-Induced Oxidative Stress Modulation with Physical Activity. *Front Physiol* 2017; **8**: 84.
7. O'Hagan KA, Cocchiglia S, Zhdanov AV, *et al.* PGC-1alpha is coupled to HIF-1alpha-dependent gene expression by increasing mitochondrial oxygen consumption in skeletal muscle cells. *Proc Natl Acad Sci U S A* 2009; **106**: 2188-2193.
8. Hatziiioanou D, Barkas G, Critselis E, *et al.* Chloride Intracellular Channel 4 Overexpression in the Proximal Tubules of Kidneys from the Spontaneously Hypertensive Rat: Insight from Proteomic Analysis. *Nephron* 2018; **138**: 60-70.
9. Kawabe K, Watanabe TX, Shiono K, *et al.* Influence on blood pressure of renal isografts between spontaneously hypertensive and normotensive rats, utilizing the F1 hybrids. *Jpn Heart J* 1978; **19**: 886-894.

10. Rettig R, Folberth CG, Graf C, *et al.* Are renal mechanisms involved in primary hypertension? Evidence from kidney transplantation studies in rats. *Klin Wochenschr* 1991; **69**: 597-602.
11. Clemitsen JR, Pratt JR, Frantz S, *et al.* Kidney specificity of rat chromosome 1 blood pressure quantitative trait locus region. *Hypertension* 2002; **40**: 292-297.
12. Rettig R. Does the kidney play a role in the aetiology of primary hypertension? Evidence from renal transplantation studies in rats and humans. *J Hum Hypertens* 1993; **7**: 177-180.
13. Heyman SN, Rosen S, Brezis M. The renal medulla: life at the edge of anoxia. *Blood Purif* 1997; **15**: 232-242.
14. Welch WJ, Baumgartl H, Lubbers D, *et al.* Nephron pO₂ and renal oxygen usage in the hypertensive rat kidney. *Kidney Int* 2001; **59**: 230-237.
15. Wang Z, Sun Q, Sun N, *et al.* Mitochondrial Dysfunction and Altered Renal Metabolism in Dahl Salt-Sensitive Rats. *Kidney Blood Press Res* 2017; **42**: 587-597.
16. de Cavanagh EM, Toblli JE, Ferder L, *et al.* Renal mitochondrial dysfunction in spontaneously hypertensive rats is attenuated by losartan but not by amlodipine. *Am J Physiol Regul Integr Comp Physiol* 2006; **290**: R1616-1625.
17. Welch WJ, Baumgartl H, Lubbers D, *et al.* Renal oxygenation defects in the spontaneously hypertensive rat: role of AT₁ receptors. *Kidney Int* 2003; **63**: 202-208.
18. Lee H, Abe Y, Lee I, *et al.* Increased mitochondrial activity in renal proximal tubule cells from young spontaneously hypertensive rats. *Kidney Int* 2014; **85**: 561-569.
19. Bhargava P, Schnellmann RG. Mitochondrial energetics in the kidney. *Nat Rev Nephrol* 2017; **13**: 629-646.
20. Biswas SK, de Faria JB. Which comes first: renal inflammation or oxidative stress in spontaneously hypertensive rats? *Free radical research* 2007; **41**: 216-224.
21. Marín-García J, Akhmedov A, Rybin V, *et al.* *Mitochondria and their role in cardiovascular disease*. Springer: New York, 2013.
22. Clayton DA. Transcription and replication of mitochondrial DNA. *Hum Reprod* 2000; **15 Suppl 2**: 11-17.
23. Pohjoismaki JL, Wanrooij S, Hyvarinen AK, *et al.* Alterations to the expression level of mitochondrial transcription factor A, TFAM, modify the mode of mitochondrial DNA replication in cultured human cells. *Nucleic Acids Res* 2006; **34**: 5815-5828.
24. Rantanen A, Gaspari M, Falkenberg M, *et al.* Characterization of the mouse genes for mitochondrial transcription factors B1 and B2. *Mamm Genome* 2003; **14**: 1-6.

25. Litonin D, Sologub M, Shi Y, *et al.* Human mitochondrial transcription revisited: only TFAM and TFB2M are required for transcription of the mitochondrial genes in vitro. *J Biol Chem* 2010; **285**: 18129-18133.
26. Metodiev MD, Lesko N, Park CB, *et al.* Methylation of 12S rRNA is necessary for in vivo stability of the small subunit of the mammalian mitochondrial ribosome. *Cell Metab* 2009; **9**: 386-397.
27. Gleyzer N, Vercauteren K, Scarpulla RC. Control of mitochondrial transcription specificity factors (TFB1M and TFB2M) by nuclear respiratory factors (NRF-1 and NRF-2) and PGC-1 family coactivators. *Mol Cell Biol* 2005; **25**: 1354-1366.
28. Yang ZF, Drumea K, Mott S, *et al.* GABP transcription factor (nuclear respiratory factor 2) is required for mitochondrial biogenesis. *Mol Cell Biol* 2014; **34**: 3194-3201.
29. Arige V, Agarwal A, Khan AA, *et al.* Regulation of Monoamine Oxidase B Gene Expression: Key Roles for Transcription Factors Sp1, Egr1 and CREB, and microRNAs miR-300 and miR-1224. *J Mol Biol* 2019; **431**: 1127-1147.
30. Koh JH, Johnson ML, Dasari S, *et al.* TFAM Enhances Fat Oxidation and Attenuates High-Fat Diet-Induced Insulin Resistance in Skeletal Muscle. *Diabetes* 2019; **68**: 1552-1564.
31. Heckmann U, Zidek W, Schurek HJ. Sodium reabsorption in the isolated perfused kidney of normotensive and spontaneously hypertensive rats. *J Hypertens Suppl* 1989; **7**: S172-173.
32. Carey RM. Blood Pressure and the Renal Actions of AT2 Receptors. *Curr Hypertens Rep* 2017; **19**: 21.
33. Zhu L, Wang Q, Zhang L, *et al.* Hypoxia induces PGC-1alpha expression and mitochondrial biogenesis in the myocardium of TOF patients. *Cell Res* 2010; **20**: 676-687.
34. Malarkey CS, Bestwick M, Kuhlwilm JE, *et al.* Transcriptional activation by mitochondrial transcription factor A involves preferential distortion of promoter DNA. *Nucleic Acids Res* 2012; **40**: 614-624.
35. Thomas JL, Pham H, Li Y, *et al.* Hypoxia-inducible factor-1alpha activation improves renal oxygenation and mitochondrial function in early chronic kidney disease. *Am J Physiol Renal Physiol* 2017; **313**: F282-F290.
36. Galvan DL, Green NH, Danesh FR. The hallmarks of mitochondrial dysfunction in chronic kidney disease. *Kidney Int* 2017; **92**: 1051-1057.
37. Wang Z, Ying Z, Bosy-Westphal A, *et al.* Specific metabolic rates of major organs and tissues across adulthood: evaluation by mechanistic model of resting energy expenditure. *Am J Clin Nutr* 2010; **92**: 1369-1377.

38. Kuhlmann U, Schwickardi M, Trebst R, *et al.* Resting metabolic rate in chronic renal failure. *J Ren Nutr* 2001; **11**: 202-206.
39. Meyer C, Nadkarni V, Stumvoll M, *et al.* Human kidney free fatty acid and glucose uptake: evidence for a renal glucose-fatty acid cycle. *The American journal of physiology* 1997; **273**: E650-654.
40. Tuma Z, Kuncova J, Mares J, *et al.* Mitochondrial proteomes of porcine kidney cortex and medulla: foundation for translational proteomics. *Clin Exp Nephrol* 2016; **20**: 39-49.
41. Queiroz-Madeira EP, Lara LS, Wengert M, *et al.* Na(+)-ATPase in spontaneous hypertensive rats: possible AT(1) receptor target in the development of hypertension. *Biochim Biophys Acta* 2010; **1798**: 360-366.
42. Li J, He Q, Wu W, *et al.* Role of the renal sympathetic nerves in renal sodium/potassium handling and renal damage in spontaneously hypertensive rats. *Exp Ther Med* 2016; **12**: 2547-2553.
43. Biollaz J, Waeber B, Diezi J, *et al.* Lithium infusion to study sodium handling in unanesthetized hypertensive rats. *Hypertension* 1986; **8**: 117-121.
44. Wu A, Wolley M, Stowasser M. The interplay of renal potassium and sodium handling in blood pressure regulation: critical role of the WNK-SPAK-NCC pathway. *J Hum Hypertens* 2019.
45. Cowley AW, Jr., Abe M, Mori T, *et al.* Reactive oxygen species as important determinants of medullary flow, sodium excretion, and hypertension. *Am J Physiol Renal Physiol* 2015; **308**: F179-197.
46. Haddock B, Larsson HBW, Francis S, *et al.* Human renal response to furosemide: Simultaneous oxygenation and perfusion measurements in cortex and medulla. *Acta Physiol (Oxf)* 2019; e13292.
47. Manotham K, Tanaka T, Matsumoto M, *et al.* Evidence of tubular hypoxia in the early phase in the remnant kidney model. *J Am Soc Nephrol* 2004; **15**: 1277-1288.
48. Adler S, Huang H. Impaired regulation of renal oxygen consumption in spontaneously hypertensive rats. *J Am Soc Nephrol* 2002; **13**: 1788-1794.
49. Farsijani NM, Liu Q, Kobayashi H, *et al.* Renal epithelium regulates erythropoiesis via HIF-dependent suppression of erythropoietin. *J Clin Invest* 2016; **126**: 1425-1437.
50. Bruschi G, Minari M, Bruschi ME, *et al.* Similarities of essential and spontaneous hypertension. Volume and number of blood cells. *Hypertension* 1986; **8**: 983-989.
51. Li H, Satriano J, Thomas JL, *et al.* Interactions between HIF-1alpha and AMPK in the regulation of cellular hypoxia adaptation in chronic kidney disease. *Am J Physiol Renal Physiol* 2015; **309**: F414-428.

52. Wang YE, Marinov GK, Wold BJ, *et al.* Genome-wide analysis reveals coating of the mitochondrial genome by TFAM. *PLoS One* 2013; **8**: e74513.
53. Ngo HB, Lovely GA, Phillips R, *et al.* Distinct structural features of TFAM drive mitochondrial DNA packaging versus transcriptional activation. *Nat Commun* 2014; **5**: 3077.
54. Pastukh VM, Gorodnya OM, Gillespie MN, *et al.* Regulation of mitochondrial genome replication by hypoxia: The role of DNA oxidation in D-loop region. *Free Radic Biol Med* 2016; **96**: 78-88.
55. Agaronyan K, Morozov YI, Anikin M, *et al.* Mitochondrial biology. Replication-transcription switch in human mitochondria. *Science* 2015; **347**: 548-551.
56. Rodriguez-Iturbe B, Quiroz Y, Ferrebuz A, *et al.* Evolution of renal interstitial inflammation and NF-kappaB activation in spontaneously hypertensive rats. *Am J Nephrol* 2004; **24**: 587-594.

TABLES

Table 1: Primers for cloning the promoter region of mitochondrial transcription factors

S.no.	Primer name	Primer sequence (5'- to 3'- direction)
1	rTfam-pro-1420-FP	CCCCGGTACCGGATATGGGATTAGGAGG
2	rTfam-pro+2-RP	CCCCCTCGAGCCAGTGTTCTTAGCACGC
3	rTfb1m-pro-1376-FP	CCCCGGTACCGGCCAGAAAATGGACAGG
4	rTfb1m-pro+4-RP	CCCCCTCGAGCTCGAATGGTGGGTAACG
5	rTfb2m-pro-1584-FP	CCCCGGTACCGGTAGAGCGCTTACCTAGG
6	rTfb1m-pro-83-RP	CCCCCTCGAGCTTCACGGCCTCACTAGG

Bolded sequences indicate the restriction sites for KpnI (GGTACC) and XhoI (CTCGAG) added in the primer sequence in order to facilitate cloning.

Table 2: HIF-1 α binding sites predicted in the promoters of mitochondrial transcription factors using various in silico tools

Gene	Location	Score				
		Matinspector	Consite	p-Match	Jaspar	Lasagna
Tfam	-174	0.75	5.75	0.80	15.61	-
	-385	-	7.10	0.80	-	9.73
	-780	-	5.75	0.80	6.18	2.80
	-1072	-	7.68	-	8.29	-
Tfb1m	-157	1.00	4.43	0.80	4.40	-
	-851	0.75	4.89	-	-	-
Tfb2m	-282	0.75	5.24	0.80	-	-
	-600	0.80	5.30	0.80	-	-

Table 3: GenBank/Ensembl accession IDs for mitochondrial transcription factors of mammals

S. No	Species	Tfam	Tfb1m	Tfb2m
1	Human	NM_003201	NM_016020	NM_022366
2	Rat	NM_031326.1	NM_181474.2	NM_001008293.1
3	Mouse	NM_009360	NM_146074	NM_008249
4	Chimp	NM_001194942.1	NM_001362392.1	ENSPTRT00000004012.2
5	Orangutan	NM_001131295.1	NM_001133415.1	-NA-
6	Gorilla	NM_001131295	NM_001292158	ENSGGOT00000001101.1
7	Rhesus Monkey	NM_001194942	NM_001261482.1	ENSMMUT00000032256.3
8	Green Monkey	NM_001130211	NM_001362392	ENCSTAT00000007204.1
9	Gibbon	ENSNLET00000015683.2	NM_ENSNLET00000037292.2	NM_ENSNLET00000005278.3
10	Macaque	ENSNFAT00000025894.1	NM_001283474.1	NM_001319608.1
11	Dog	ENSCAFT00000038143.2	NM_ENSCAFT00000000895.3	-NA-
12	Pig	ENSSSCT00000046982.1	NM_001128475.1	ENSSSCT00000032587.2
13	Cow	NM_001034016.2	NM_001076896.2	NM_001038127.2

Table 4: Primers used for real time PCR to quantify various mitochondrial genes

S.no.	Gene		Primer sequence (5'-3')	Annealing Temp (°C)	Product Size
1	Tfam	FP	TGTCAGCCTTATCTGTATTCC	55	129
		RP	TTTGCATCTGGGTGTTTAG		
2	Tfb1m	FP	CGCGTGTGTATGTAGGTCTCA	55	187
		RP	TCTGCTAGACTGCCAGCTTTC		
3	Tfb2m	FP	CGTAGCTTCTCTGACCTCTACA	55	200
		RP	ATTCCTGGACCTGGATTG		
4	16S rRNA	FP	AACTCGGCAAACAAGAACCC	55	152
		RP	CCCTAATTAAGGAACAAGTG		
5	ND5	FP	CTCCACATTTGCACCCATG	62	171
		RP	TATTCCGGTAAGGGCTAGG		
6	ND6	FP	GTCTAGGGTTGGCGTTGAAG	55	184
		RP	TCCTCAGTAGCCATAGCAG		
7	HIF-1 α	FP	GTTTACTAAAGGACAAGTCACC	62	193
		RP	TTCTGTTTGTGTAAGGGAG		
8	PGC-1 α	FP	CCCCAGGCAGTAGATCCTC	62	125
		RP	CCTACGGCTGTAGGGTGAC		
9	β Actin	FP	GCTGTGCTATGTTGCCCTAG	55	117
		RP	CGCTCATTGCCGATAGTG		
10	18S rRNA	FP	GGATCCATTGGAGGGCAAGT	55	91
		RP	ACGAGCTTTTAACTGCAAGCAA		

Table 5: Conditions for Western blotting

S.no	Antibody	Blocking	Primary Antibody	Secondary antibody
1	Tfam	Overnight at 4°C with 1% PVP	1:7500 1 hour at RT	1:5000 (Rabbit IgG)
2	Tfb1m	Overnight at 4°C with 1% PVP	1:5000 1 hour at RT	1:3000 (Rabbit IgG)
3	Tfb2m	Overnight at 4°C with 1% PVP	1:5000 1 hour at RT	1:3000 (Goat IgG)
4	HIF1 α	2 hours at RT with 5% skim milk	1:2500 Overnight at 4°C	1:3000 (Mouse IgG)
5	PGC1 α	1 hour at RT with 5% skim milk	1:3000 Overnight at 4°C	1:3000 (Rabbit IgG)
6	OXPPOS cocktail	1 hour at RT with 5% skim milk	1:400 Overnight at 4°C	1:4000 (Rabbit IgG)
7	Vinculin	1 hour at RT with 3% BSA	1:10000 Overnight at 4°C	1:5000 (Mouse IgG)

Table 6: Primers used for Chromatin Immunoprecipitation

S.no.	HRE Location		Primer sequence (5'-3')	Annealing Temp (°C)	Product Size
1	Tfam HRE 1&2	FP	GATTTCAAGAGCCACGCAC	57.1	275
		RP	AGACTTCCGGTCTGCAGC		
2	Tfam HRE 3	FP	CCGGATGAATGAGACGGTTG	55	140
		RP	CAGGTTGGTGGTGCAAACC		
3	Tfam HRE 4	FP	CTCTGCGGCTTGAAGGAG	55	150
		RP	TGAGATCCTAACAACAACAGCC		
4	Tfb1m HRE 1	FP	TCTCCTAGACTCCGCCTCCT	55	207
		RP	GAGACCTACATACACACGCG		
5	Tfb1m HRE 2	FP	GCATGCTATGGCTGGATGTA	62	133
		RP	ATGACTCCCTTTCCCCTCC		
6	Tfb2m HRE 1	FP	CCGCACTGGAGAATCAGAC	55	150
		RP	TCCGGGCTGGAAGTCTATG		
7	Tfb2m HRE 2	FP	ACACCGACGCGGAGTAGA	62	190
		RP	GGAGAGTCGTTGGCTCCTC		
8	16S rRNA*	FP	AACTCGGCAAACAAGAACCC	55	152
		RP	CCCTAATTAAGGAACAAGTG		
9	ND5*	FP	CTCCACATTTGCACCCATG	62	171
		RP	TATTCCGGTAAGGGCTAGG		

- *- denotes the same primers used for mRNA expression analysis of these genes.

FIGURES

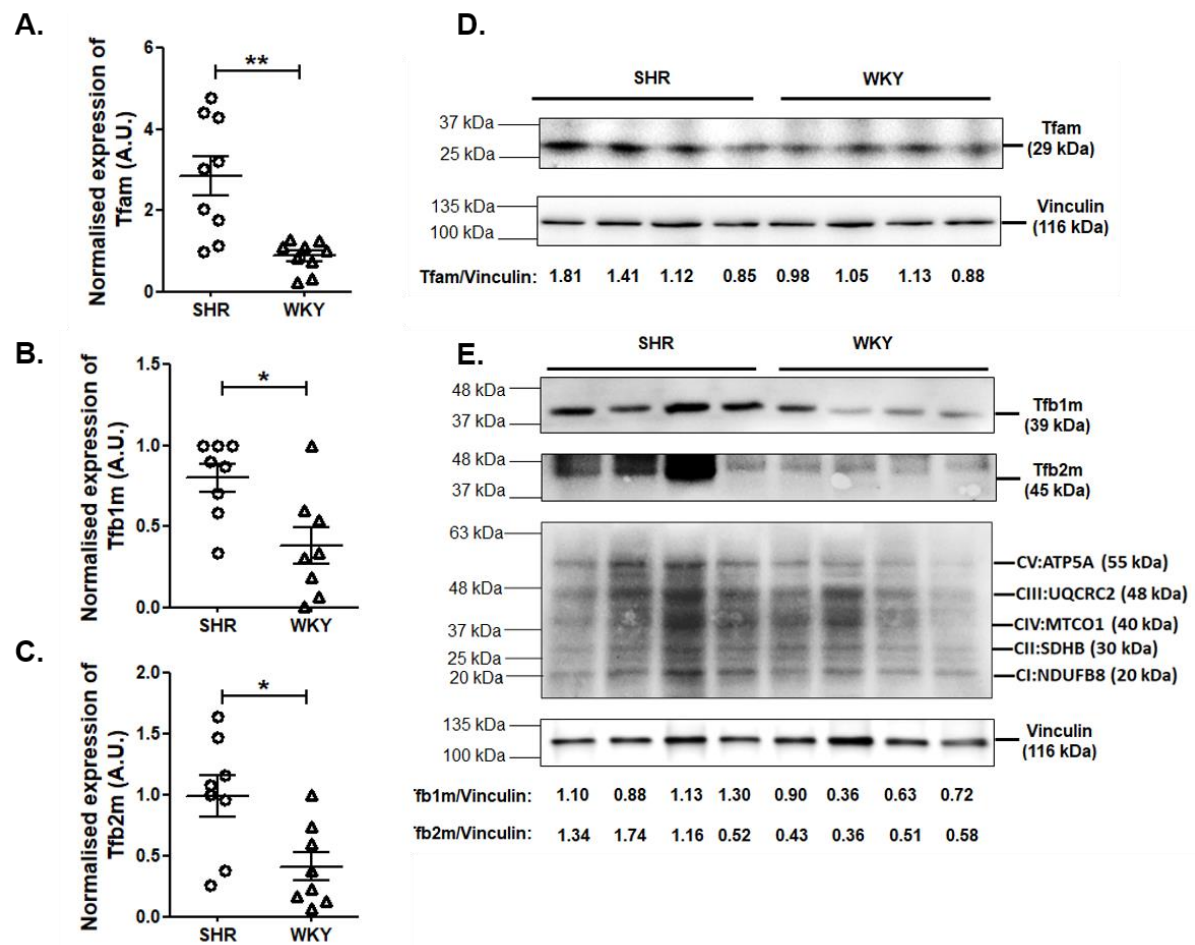


Figure 1. Endogenous expression of mitochondrial transcription factors in SHR/WKY kidney: Total RNA and protein were isolated from kidney tissue homogenates of SHR and WKY. RNA was subjected to reverse transcription and 40 ng of cDNA was used in qPCR reaction to estimate endogenous transcript levels of (A) Tfam, (B) Tfb1m and (C) Tfb2m using gene specific primers. Normalisation was carried out with respect to expression of β -Actin. Unpaired, 2-tailed Student's T-test was used statistical analysis. ** represents $p < 0.005$ and * represents $p < 0.05$. Western blot was done using kidney homogenates from SHR and WKY. Representative images are shown for (D) Tfam, (E) Tfb1m, Tfb2m and OXPHOS. Vinculin was used as a loading control for Western blot and the corresponding normalised densitometric quantifications are shown below the images.

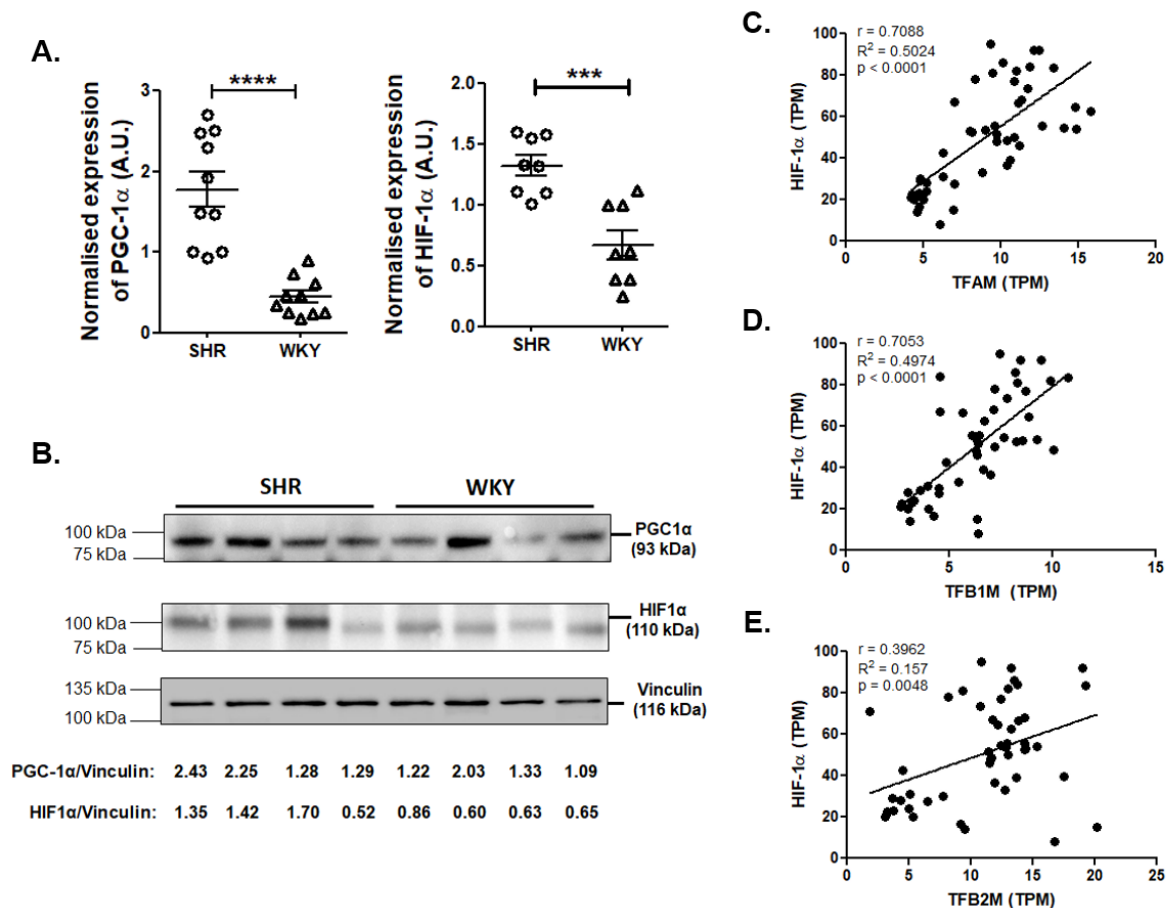


Figure 2. Endogenous expression of HIF-1 α and PGC-1 α in SHR/WKY kidney and correlation between expression of HIF-1 α and mtTFs: (A) Total RNA and protein were isolated from kidney tissue homogenates of SHR and WKY. RNA was subjected to reverse transcription and 40 ng of cDNA was used in qPCR reaction to estimate endogenous transcript levels of HIF-1 α and PGC-1 α , using gene specific primers. Normalisation was carried out with respect to expression of β -Actin. Unpaired, 2-tailed Student's T-test was used statistical analysis. **** represents $p < 0.0001$ and *** represents $p < 0.001$. (B) Western blot was done using kidney homogenates from SHR and WKY. Representative images are shown for HIF-1 α and PGC-1 α . Vinculin was used as a loading control for Western blot. Correlation between the expression of HIF-1 α and (D) Tfam, (E) Tfb1m and (F) Tfb2m in various human tissues was plotted using transcriptomic data from the GTex portal.

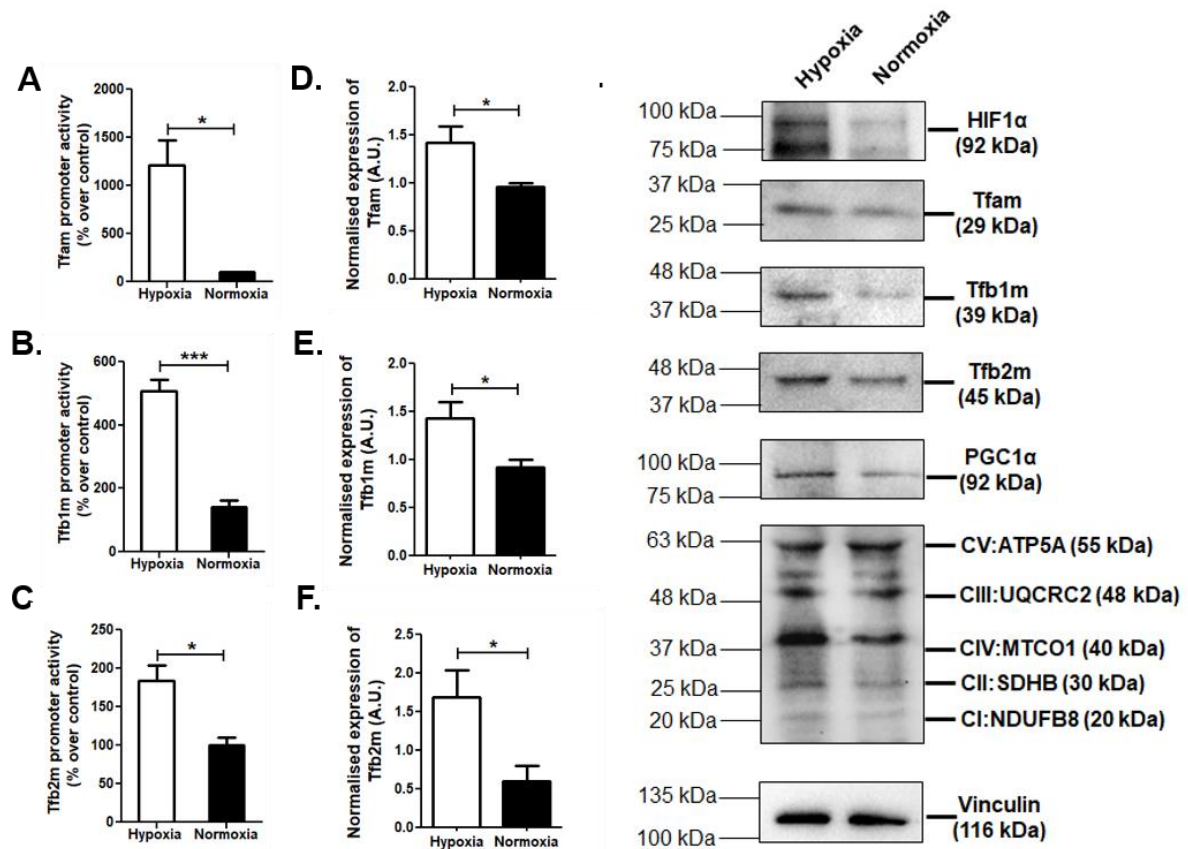


Figure 3. Effect of acute hypoxia on the promoter activity, mRNA and protein expression of mitochondrial transcription factors in NRK52e cells: (A-C) NRK52e cells transfected with promoter luciferase-reporter constructs of (A) Tfam, (B) Tfb1m or (C) Tfb2m were subjected to acute hypoxia for two hours and luciferase activity indicating promoter activity was measured. Results are expressed as percentage over control after normalisation with β -galactosidase activity as a transfection control and total protein as a control for number of cells. mRNA expression of (D) Tfam, (E) Tfb1m or (F) Tfb2m were estimated through qPCR after NRK52e cells were subjected to acute hypoxia. (G) Representative Western blots showing protein levels of Tfam, Tfb1m, Tfb2m, HIF-1 α , PGC-1 α and total OXPHOS after acute hypoxia are shown. Student's T-test (unpaired, two-tailed) was used for determining the statistical significance of the changes in expression after hypoxia. * represents $p < 0.05$ and ** represents $p < 0.001$ with respect to the normoxic condition.

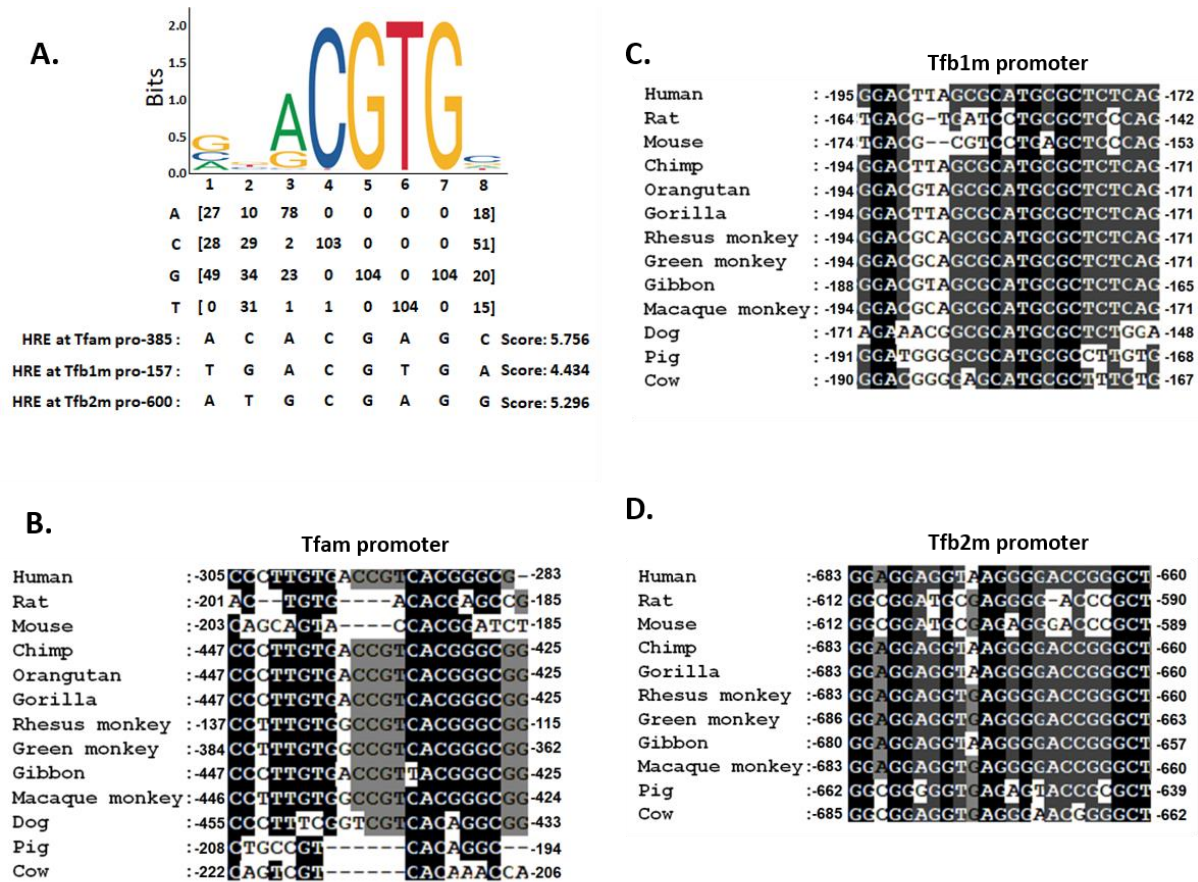


Figure 4. Conserved HIF-1α binding sites in the promoter regions of mitochondrial transcription factors: (A) Position weight matrices for HIF-1α obtained from Jaspar is shown. The promoters of mitochondrial transcription factors were analysed in silico using various online tools for the presence of Hypoxia Response Elements (HREs). The promoter sequence of Tfam, Tfb1m and Tfb2m where HREs predicted are shown below the matrix. The score for each of these sites as obtained from Consite is indicated for each respective promoter sequences. Out of multiple HREs predicted for these promoters, one was conserved for each and this conservation among mammals is represented in (B) Tfam, (C) Tfb1m and (D) Tfb2m.

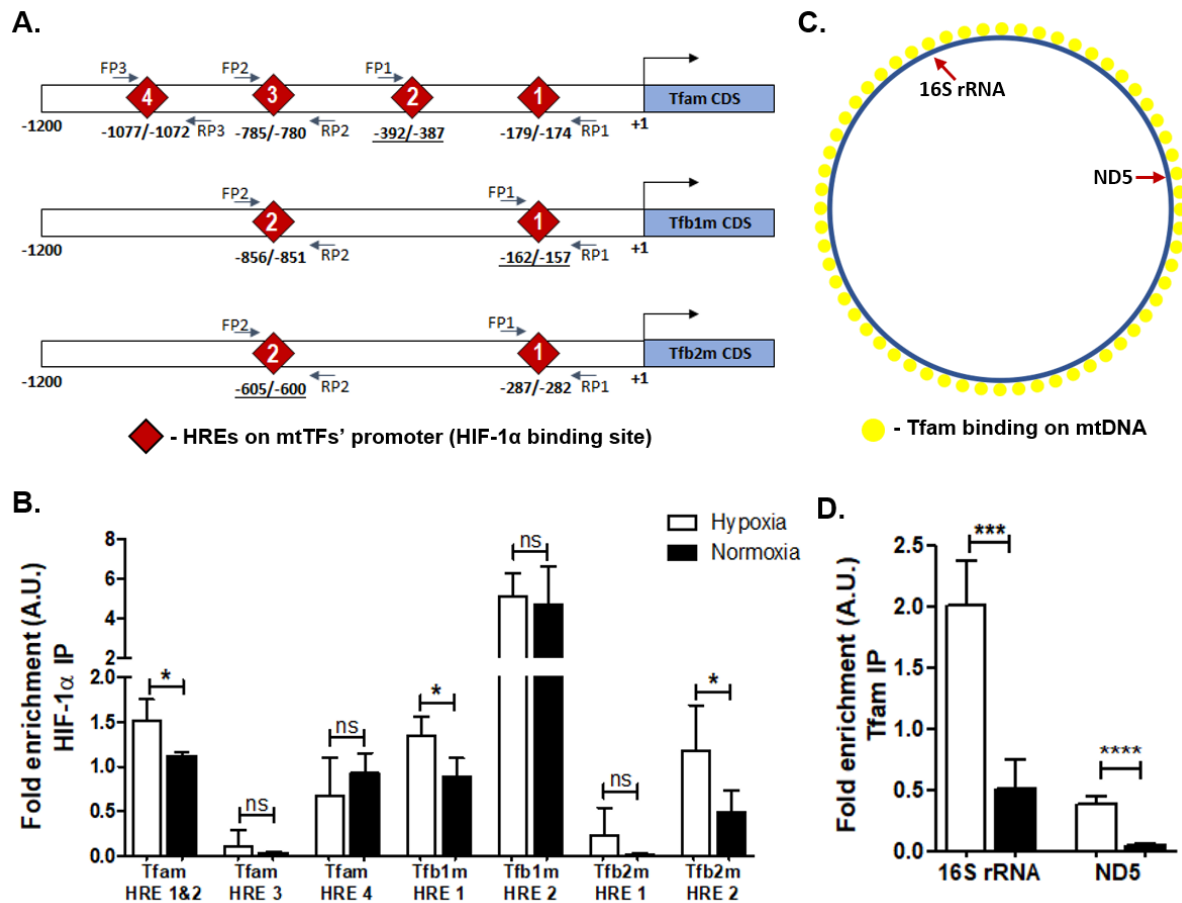


Figure 5. In-vivo interaction of HIF1α and Tfam with mtTFs promoters and mtDNA respectively: (A) Schematic representation of HIF-1α binding sites on the promoters of mtTFs. the primers flanking each of these binding sites are indicated as arrows. Bold and underlined sites denote conserved HREs. (C) Schematic representation of Tfam binding sites on mtDNA. Positions of 16S rRNA and ND5 genes are indicated. NRK52e cells were subjected to acute hypoxia for two hours. Chromatin was reverse crosslinked and fragmented prior to immunoprecipitation with HIF-1α and Tfam antibodies. The immunoprecipitated DNA was subjected to qPCR analysis using primers flanking various HREs (B) or mtDNA genes (D) was done to assess the binding of HIF-1α and Tfam respectively. Students t-Test was used to determine the statistical significance of differential binding. * represents p < 0.05 and *** indicates p < 0.001 with respect to the normoxic condition.

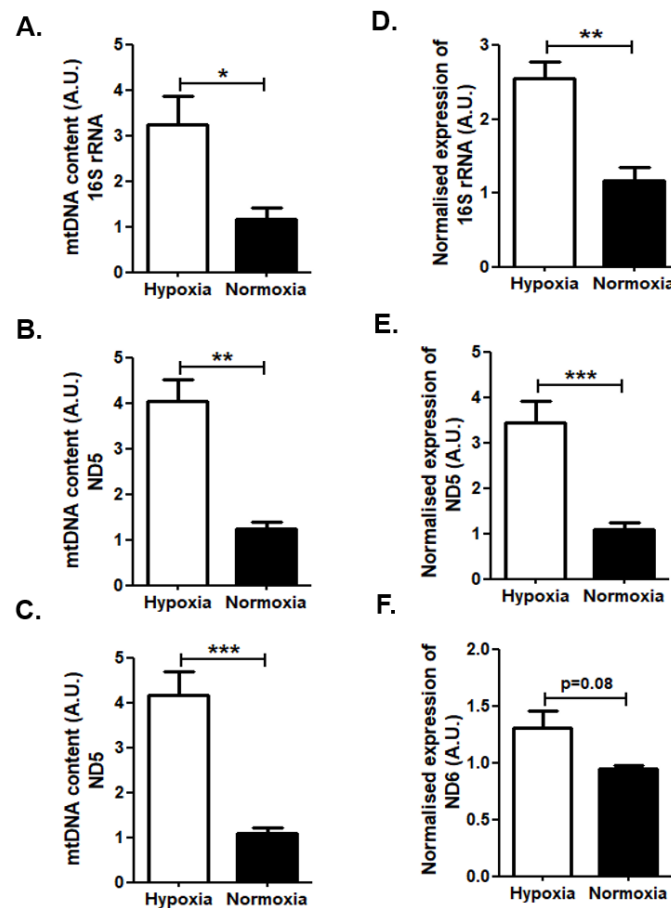


Figure 6. Effect of acute hypoxia on the expression of mtDNA and mtRNA: NRK52e cells were subjected to acute hypoxia for two hours and DNA, RNA and protein were isolated. Real-time qPCR was performed using primers specific for three mitochondrial genes using genomic DNA as template and primers specific for (A) 16S rRNA, (B) ND5 and (C) ND6 and normalised with 18S rRNA. (D-F) Similar analysis was performed using total cDNA as template and normalised with β -Actin to estimate mtRNA (D) 16S rRNA, (E) ND5 and (F) ND6. Student's T-test (unpaired, two-tailed) was used for determining the statistical significance of the changes in expression after hypoxia. * represents $p < 0.05$, ** represents $p < 0.01$ and *** indicates $p < 0.001$ with respect to the normoxic condition.

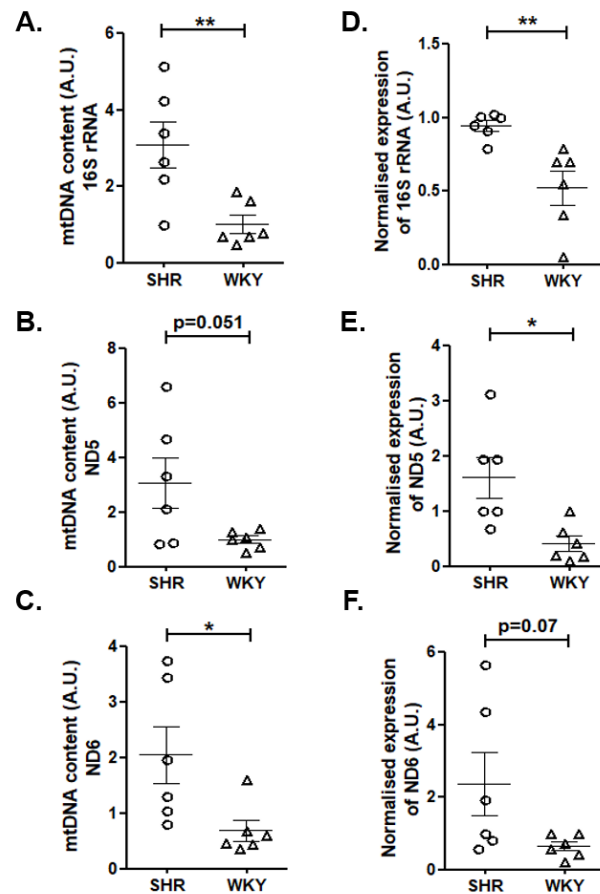


Figure 7. Expression of mtDNA and mtRNA in kidney tissue of SHR and WKY: Real-time qPCR analysis was performed using genomic DNA and total cDNA from kidney tissues of SHR and WKY for quantifying (A-C) mtDNA and (D-F) mtRNA respectively. Primers were used against three mitochondrial genes (A&D) 16S rRNA, (B&E) ND5 and (C&F) ND6 and normalised with 18S rRNA for mtDNA and β -Actin for mtRNA. Student's T-test (unpaired, two-tailed) was utilized to determine the statistical significance of differential expression. * represents $p < 0.05$, ** represents $p < 0.01$ with respect to WKY.

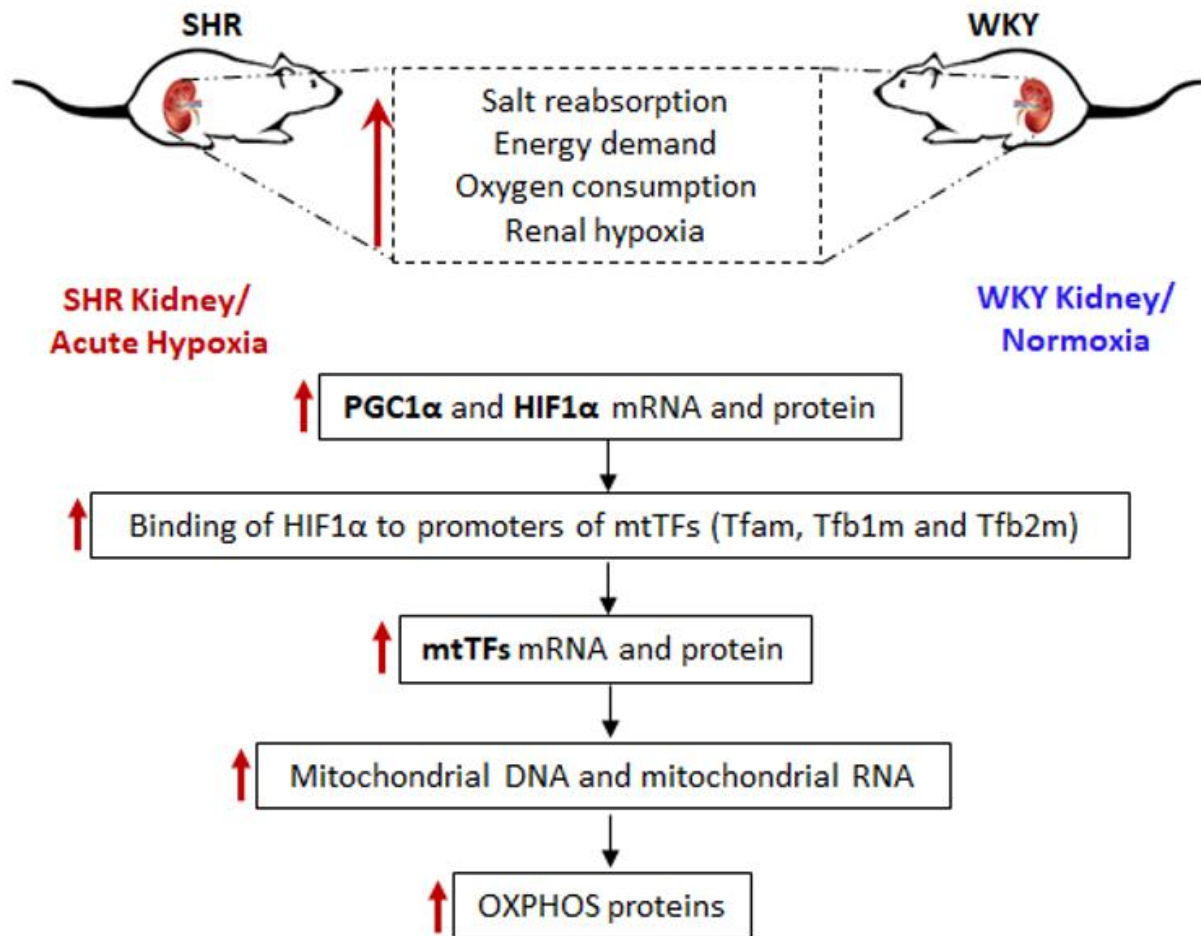


Figure 8: Plausible mechanisms of regulation of mitochondrial transcription factors during acute hypoxia and in hypertensive renal physiology. Hypoxic SHR kidneys and NRK52e cells subjected to acute hypoxia display augmented expression of mitochondrial transcription factors. HIF-1α mediates the increase in expression of mtTFs at the transcriptional level. Augmented mtTFs result in increase in mtDNA and mtRNA levels leading to enhanced OXPHOS expression.